Note: Equation of state and the freezing point in the hard-sphere model

Miguel Robles,[1,a)] Mariano López de Haro,[1,b)] and Andrés Santos[2,c)]
[1]*Instituto de Energías Renovables, Universidad Nacional Autónoma de México (U.N.A.M.), Temixco, Morelos 62580, Mexico*
[2]*Departamento de Física, Universidad de Extremadura, Badajoz E-06071, Spain*

(Received 10 January 2014; accepted 25 March 2014; published online 3 April 2014)

[http://dx.doi.org/10.1063/1.4870524]

Despite the simplicity of the hard-sphere (HS) intermolecular potential and the vast amount of studies devoted to this model, up to date no one has been able to derive analytically neither the free energy nor the phase diagram of the HS system. Therefore, many of the important results concerning the equilibrium properties of the HS model have been obtained from computer simulations. It is well known that in the HS system the absolute temperature T only enters as a scaling parameter and so its equation of state (EOS) is usually presented as a graph in the compressibility factor ($Z \equiv p/\rho k_B T$, with p, ρ, and k_B being the pressure, number density, and Boltzmann constant, respectively) vs packing fraction ($\eta \equiv \frac{\pi}{6}\rho\sigma^3$, σ being the diameter of the spheres) plane.[1] The characteristics of this diagram are relatively well understood, at least qualitatively. It comprises a stable fluid branch going from $\eta = 0$ to the freezing packing fraction $\eta_{\rm f} \simeq 0.492$, where a fluid-solid phase transition takes place,[2,3] a region of fluid-solid coexistence from $\eta_{\rm f}$ to the crystal melting point $\eta_{\rm m} \simeq 0.543$,[3,4] and finally a stable solid (crystalline) branch from $\eta_{\rm m}$ to the close-packing fraction $\eta_{\rm cp} = \frac{\pi}{6}\sqrt{2} \simeq 0.7405$.[5] Beyond the freezing point there is also a region of metastable fluid states that is supposed to end at the packing fraction $\eta_{\rm g} \simeq 0.58$,[5,6] where a widely accepted glass transition occurs. The glass branch ends at $\eta_{\rm rcp} \simeq 0.64$ corresponding to the random close-packing of an amorphous solid.[7] There is further a region of metastable crystalline states for packing fractions below $\eta_{\rm m}$.

Recently, accurate tethered Monte Carlo (MC) simulations have been reported[3] in which the fluid-solid coexistence pressure ($p_{\rm coex}$) of the HS system was computed, namely, $p^*_{\rm coex} \equiv (\sigma^3/k_B T)p_{\rm coex} = 11.5727(10)$, the number enclosed by parentheses denoting the statistical error. The specific volumes associated with the freezing and melting points were also reported with the values $v_{\rm f} = 1/\rho_{\rm f} = 1.06448(10)\sigma^3$ and $v_{\rm m} = 1/\rho_{\rm m} = 0.96405(3)\sigma^3$, respectively.

Given these results, the aim of this Note is to explore whether starting with the above high-accuracy estimate of $p_{\rm coex}$ and determining the freezing-point packing fraction (with its associated statistical error) from available analytical EOS one may conclude which one yields the best performance near the freezing point. To achieve our goal, we will examine the following four analytical EOS. First, we recall the celebrated Carnahan–Starling (CS)[8] EOS:

$$Z_{\rm CS} = \frac{1+\eta+\eta^2-\eta^3}{(1-\eta)^3}. \tag{1}$$

Next, we consider Kolafa's correction, i.e., the Carnahan–Starling–Kolafa (CSK)[9] EOS:

$$Z_{\rm CSK} = \frac{1+\eta+\eta^2-\frac{2}{3}(1+\eta)\eta^3}{(1-\eta)^3}. \tag{2}$$

As a third EOS, a proposal based on the so-called rescaled virial (RV) expansion[10] will also be included, namely,

$$Z_{\rm RV} = \frac{1+\sum_{n=1}^{6} C_n \eta^n}{(1-\eta)^3}, \tag{3}$$

with $C_1 = C_2 = 1$, and $C_n = \sum_{j=0}^{3}\binom{3}{j}(-1)^{j+1} b_{n-2+j}$ for $n = 3$–6, b_j being the (reduced) virial coefficients. Finally, a recently proposed branch-point (BP) approximant[11] will be considered. It reads

$$Z_{\rm BP} = 1 + \frac{1+\sum_{n=1}^{3} c_n \eta^n - (1+2a_1\eta+a_2\eta^2)^{3/2}}{A(1-\eta)^3}, \tag{4}$$

with $a_1 = -C_5/C_4$, $a_2 = 7a_1^2 - 6C_6/C_4$, $A = -\frac{3}{8}(a_2 - a_1^2)^2/C_4$, $c_1 = 3a_1 + 4A$, $c_2 = \frac{3}{2}(a_2 + a_1^2) - 2A$, and $c_3 = \frac{1}{2}a_1(3a_2 - a_1^2) + (b_4 - 18)A$. One should add in connection with Eqs. (3) and (4) that they require the first seven virial coefficients. Only $b_2 = 4$, $b_3 = 10$, and $b_4 = \frac{219\sqrt{2} - 712\pi + 4131\tan^{-1}\sqrt{2}}{35\pi}$ are exactly known, while $b_5 = 28.22445(10)$, $b_6 = 39.81550(36)$, and $b_7 = 53.3413(16)$ have been determined numerically.[12]

The procedure involves inverting Eqs. (1)–(4) to compute $\eta_{\rm f}$ (and its statistical error $\Delta\eta_{\rm f}$) from the MC value of $p^*_{\rm coex}$ (and its associated statistical error $\Delta p^*_{\rm coex} = 10^{-3}$). The four EOS give $\partial p^*/\partial\eta|_{\eta=0.492} \approx 100$–$101$, so that one can easily estimate $\Delta\eta_{\rm f} \approx 10^{-5}$. However, although the numerical inversion of Eqs. (1) and (2) is straightforward, there are complications associated with Eqs. (3) and (4) due to the statistical uncertainties on the higher order virial coefficients. To take these into account we used the following procedure. (i) A random number p^* is generated having a normal distribution with average value $p^*_{\rm coex}$ and standard deviation $\Delta p^*_{\rm coex} = 10^{-3}$; (ii) a value of the packing fraction η is derived through the equation $\frac{6}{\pi}\eta Z(\eta) = p^*$, where $Z(\eta)$ is the compressibility factor corresponding to each one of the above EOS; (iii) step (i) is

a)Electronic mail: mrp@ier.unam.mx. URL: http://xml.ier.unam.mx/xml/tc/ft/mrp/.
b)Electronic mail: malopez@unam.mx. URL: http://xml.ier.unam.mx/xml/tc/ft/mlh/.
c)Electronic mail: andres@unex.es. URL: http://www.unex.es/eweb/fisteor/andres/.

TABLE I. Freezing-point packing fraction η_f as measured in tethered MC simulations[3] and as derived from Eqs. (1)–(4) and from a fit to MD simulation data.[13] The third column provides the excess chemical potential at the freezing point, $\beta\mu_f^{ex}$, as derived from Eqs. (1)–(4) and from a fit to MC simulation data.[14]

Method	η_f	$\beta\mu_f^{ex}$
Tethered MC[a]	0.491882(46)	...
CS	0.491972(10)	16.1119(11)
CSK	0.491927(10)	16.1395(10)
RV	0.491820(10)	16.1404(11)
BP	0.491917(10)	16.1289(11)
MD[b] and MC[c]	0.491835(11)	16.167(54)

[a]Reference 3.
[b]Reference 13.
[c]Reference 14.

repeated so as to gather a statistically representative set of $\mathcal{N}$ values of η; and (iv) finally, η_f is taken as the average of the above solutions and the standard deviation $\Delta\eta_f$ is equated to the associated statistical error. In the cases of Eqs. (3) and (4) we also accounted for the statistical errors associated with b_5–b_7 in the MC procedure, but we observed that their influence was practically negligible. The number of elements were chosen as $\mathcal{N} = 5 \times 10^4$ for Eqs. (1) and (2) and $\mathcal{N} = 1.5 \times 10^5$ for Eqs. (3) and (4).

After applying the previous procedure to each one of the EOS (1)–(4), the results shown in the second column of Table I were obtained. The simulation value of η_f that follows from the value of the freezing-point specific volume v_f stated earlier is also included in Table I. Additionally, Table I contains an estimate of η_f obtained by application of the procedure outlined above to a quadratic fit to recent rather accurate molecular dynamics (MD) simulation data, together with their error bars,[13] for the three closest densities ($\rho\sigma^3 = 0.930$, 0.940, and 0.950) to the freezing density.

The results of Table I for η_f are graphically displayed in Fig. 1. It is clear that the best performance with respect to the simulation results is provided by both Z_{CSK} and Z_{BP}, with possibly a slight superiority of the latter. Whereas Z_{CSK} is simpler than Z_{BP}, the latter has the advantage of predicting a physical value (smaller than η_{cp}) for the radius of convergence of the virial series.[11,15] It is also interesting to note that the MD estimate and the MC value of η_f are statistically consistent since the difference between them is slightly smaller than the combined standard deviation.

It might be argued that using a single density–pressure point at freezing is not sufficient for a fair assessment of the whole stable fluid branch. To account for this, we have also analyzed the excess chemical potential at freezing, $\beta\mu_f^{ex} = Z(\eta_f) - 1 + \int_0^{\eta_f} d\eta'[Z(\eta') - 1]/\eta'$, which requires integration over the whole fluid range. We have evaluated $\beta\mu_f^{ex}$ from Eqs. (1)–(4) by following a procedure similar to the one described above (with $\mathcal{N} = 1.5 \times 10^5$), except that the values of η_f along with their uncertainties are now used. The results are displayed in the third column of Table I. Since $\beta\mu_f^{ex}$ was not directly reported in Ref. 3, we have resorted to MC results of Ref. 14 for $\rho\sigma^3 = 0.925$, 0.94, and 1.0 and applied our procedure (again with $\mathcal{N} = 1.5 \times 10^5$) to a quadratic fit. Except in the CS case, the theoretical values deviate from the MC estimate less than the combined standard deviation. In any case, a more accurate simulation value for $\beta\mu_f^{ex}$ would be needed to discriminate among the CSK, RV, and BP predictions.

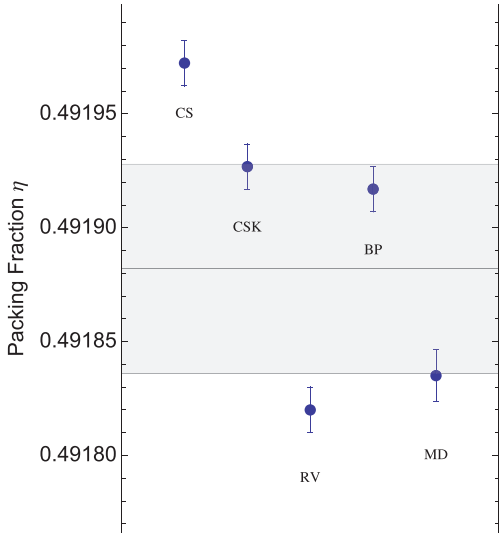

FIG. 1. Values of the HS freezing-point packing fraction η_f, together with their error bars, as obtained from Eqs. (1)–(4) and from the quadratic fit to MD data.[13] The shaded area represents the error bar corresponding to the simulation result of Ref. 3.

Two of us (A.S. and M.L.H.) acknowledge the financial support of the Spanish Government through Grant No. FIS2010-16587 and the Junta de Extremadura (Spain) through Grant No. GR10158 (partially financed by FEDER funds).

[1]*Theory and Simulation of Hard-Sphere Fluids and Related Systems*, Lectures Notes in Physics Vol. 753, edited by A. Mulero (Springer-Verlag, Berlin, 2008).
[2]B. J. Alder and T. E. Wainwright, J. Chem. Phys. **27**, 1208 (1957).
[3]L. A. Fernández, V. Martín-Mayor, B. Seoane, and P. Verrocchio, Phys. Rev. Lett. **108**, 165701 (2012).
[4]W. G. Hoover and F. H. Ree, J. Chem. Phys. **49**, 3609 (1968).
[5]R. J. Speedy, Mol. Phys. **95**, 169 (1998).
[6]G. Parisi and F. Zamponi, Rev. Mod. Phys. **82**, 789 (2010).
[7]J. Bernal and J. Mason, Nature (London) **188**, 910 (1960).
[8]N. F. Carnahan and K. E. Starling, J. Chem. Phys. **51**, 635 (1969).
[9]This EOS is a slight modification by J. Kolafa of the CS EOS. It first appeared as Eq. (4.46) in the review paper by T. Boublík and I. Nezbeda, Collect. Czech. Chem. Commun. **51**, 2301 (1986).
[10]M. Baus and J. L. Colot, Phys. Rev. A **36**, 3912 (1987).
[11]A. Santos and M. López de Haro, J. Chem. Phys. **130**, 214104 (2009).
[12]S. Labík, J. Kolafa, and A. Malijevský, Phys. Rev. E **71**, 021105 (2005).
[13]M. N. Bannerman, L. Lue, and L. V. Woodcock, J. Chem. Phys. **132**, 084507 (2010).
[14]S. Labík and W. R. Smith, Mol. Simul. **12**, 23 (1994).
[15]N. Clisby and B. M. McCoy, J. Stat. Phys. **122**, 15 (2006).